Journal of Ceramic Processing Research. Vol. 18, No. 4, pp. 275~279 (2017)

J O U R N A L O F
Ceramic Processing Research

Tailoring the microstructure of Al_2O_3-SiO_2 porous ceramics through starch consolidation by direct foaming

Woo Young Jang[a], Dong Nam Seo[a], Bijay Basnet[a], Jung Gyu Park[a], In Sub Han[b] and Ik Jin Kim[a,*]

[a]*Institute of Processing and Application of Inorganic Materials, (PAIM), Department of Advanced Materials Science and Engineering, Hanseo University, 46, Hanseo 1-ro, Haemi-myun, Seosan-si, Chungchungnam-do 31962, Korea*

[b]*Energy materials Lab., Korea Institute of Energy Research (KIER), #152 Gajeong-gu, Daejeon 305-343*

This study reports the tailoring of the microstructure of porous ceramics from particle stabilized colloidal suspension with the addition of starch by direct foaming. The initial colloidal suspension of Al_2O_3-SiO_2 was partially hydrophobized by surfactant, propyl gallate (2 wt.%) to stabilize wet foam with the addition of SiO_2 as stabilizer. The influence of the starch consolidation and solid content on the bubble size, pore size and pore distribution in terms of the contact angle, surface tension, adsorption free energy and Laplace pressure are discussed in this paper. The results show the wet foam stability of more than 85% corresponds to a particles free energy of 2.6×10^{-12} J and pressure difference of 6.0 mPa for colloidal particles with 1.25 wt. % of starch content. The uniform distribution of tri-modal micro pores were controlled by increasing starch contents and thick struts (films in wet foams), which led via higher stability wet foams to porous ceramics.

Key words: Colloidal suspension, Starch, Wet foam stability, Tailoring microstructure, Porous ceramics.

Introduction

Considering the ubiquitous presence of porous materials, tailoring the microstructure of porous ceramics from particle-stabilized wet foams by direct foaming has the potential to broaden the range of materials used in high performance applications, such as catalytic carrier, bone transplant, thermal and electrical insulation, and molten metal filters [1-2]. Direct foaming is particularly suited to the tailoring of open and closed pore structure with porosities ranging from 45 to 85%, and cell sizes between 30 μm and 1 mm. This method involves the incorporation of an air or gas bubble into a colloidal suspension of ceramic powder, solvent, surfactant, polymeric binder and gelling agents. The incorporation of the air bubble is carried out either through mechanical frothing, injection of a gas steam, gas releasing chemical reaction, or solvent evaporation [3-5].

However, in all these applications, the thermodynamic instability of liquid foams is a critical issue. Foam instability arises from the high energy associated with the gas-liquid interface. This constitutes a driving force for decreasing the foam total interface area through the coalescence and disproportionation (Ostwald ripening) of bubbles [6-7]. To improve the stability of wet foams, surfactants are used to lower the surface tension of the gas-liquid interface, and thus increase the lifetime of gas bubbles to tailor the final microstructure of porous ceramics [8-9]. The stability of the wet foams can be evaluated, as the Young-Laplace pressure links the capillary pressure and geometry. The Laplace pressure is the pressure difference between the inner and outer surface of a bubble or droplet, the effect of which is caused by the surface tension of the interface between liquid and gas [10-11].

To tailor the cellular microstructure of ceramics, our new processing route combined starch consolidation with the recently developed surface-modified particles direct foaming. Starch can not only be used as a body-foaming agent of ceramic suspension when the system is heated between 50 and 85 °C, but also provides open pores of different diameter to the microstructure of ceramics at high temperature after burning [12-14]. Sintering burns out the starch molecules, which leave the spaces behind as pores.

This study discusses the stability of the colloidal suspension as a function of Contact angle, surface tension, air content, average bubble size, adsorption free energy, Laplace pressure, foam stability and Relative bubble size with the consolidation of starch into the colloidal suspension. Particles with a starch stabilize the wet foams, and the wet foams were dried at room temperature and were sintered in argon at 1300 °C for 1 hr to tailor the microstructure of the porous ceramics. The microstructure of the cellular ceramics was characterized via FE-SEM, where pore morphology, porosity and pore size distribution were analyzed.

*Corresponding author:
Tel : +82-41-660-1441
Fax: +82-41-660-1402
E-mail: ijkim@hanseo.ac.kr

Experimental

Materials

The raw materials used in preparing the Al_2O_3 suspension were (i) α-Al_2O_3 powder (KC, South Korea, 0.4 mm and density of 3.95 g/cm^3); (ii) SiO_2 powder (Junsei Chemicals Co. Ltd, Japan 0.2 mm and density of 2.19 g/cm^3); and (iii) starch (Sigma-Adlich Chemicals GmbH, Switzerland) as pore former used to prepare the starch consolidated wet foam. The short chain carboxylic acid was used for surface modification was Propyl gallate (Fluka Analytical, Germany). Further chemicals used for this study were 10 (M) HCl (Yakuri pure Chemicals, Osaka, Japan), 4 (M) NaOH solutions (Yakuri pure Chemicals, Kyoto, Japan) for pH adjustments, and double deionized water for suspension preparation and volume adjustment.

Preparation of colloidal suspension and wet foam

α-Al_2O_3 powder and SiO_2 powder were added to de-ionized water, and separately prepared aqueous suspension. Homogenization and de-agglomeration of suspension was carried out in a ball mill for at least 48 hrs at a rotation speed of 60 rpm using polyethylene bottles and zirconia balls (10 mm in diameter), with ball/powder mass ratio 2 : 1. After ball milling, 0.2 wt. % of the propyl gallate was added as a surface modifier. The mixing speed was kept constant at 500 rpm, and the amphiphile was added as concentrate; no prior dissolution was carried out. The pH of the suspension was adjusted to 4.75 by adding NaOH and/or HCl drop wise. The solid content of the final aqueous suspension was set to 30 vol. %, by adding the required amount of water. Then, the starch consolidation was homogenized in combination with the process of in situ foaming. Then the particle stabilized suspension was foamed by mechanical frothing under observation for at least 30 min. Fig. 1 shows a schematic of the experimental procedure. Thus obtained wet foams were transferred into cylindrical molds, and left them to dry at room temperature (22-25 °C) for minimum of 24-48 hrs. After drying, the specimens were sintered in a Super Kanthal furnace (max 1650 °C) at 1300 °C for 1 hr. The heating and cooling rate were set to 1 and 3 °C/min, respectively.

Characterization

Surface tension and contact angle of the final suspension was analyzed with pendant drop method (KSV Instruments Ltd, Helsinki, Finland). The drop volume was managed within the range of 5-10 ml, for amphiphile-containing suspension.

The energy of attachment or free energy gained (G) by the adsorption of a particle of radius (r) at the interface can thus be calculated using the following equation:

$$DG = \pi r^2 \gamma_{\alpha\beta}(1-\cos\theta)^2 \quad \text{where, } \theta < 90^\circ \qquad (1)$$

where γ is the surface tension of the suspension and θ is the contact angle. The foaming of the final suspension was carried out at room temperature, and it was achieved by using a household hand mixer (150 W, Super Mix, France) at its highest power for 15 min. The mechanical frothing facilitated the air incorporation throughout the whole volume of the suspension.

Air content was calculated by the percentage of volume increase of the suspension after foaming.

$$Air\ content = \frac{(V_{wet\ foam} - V_{suspension}) \times 100}{V_{wet\ foam}} \qquad (2)$$

where, $V_{wet\ foam}$ indicates the wet foam volume after

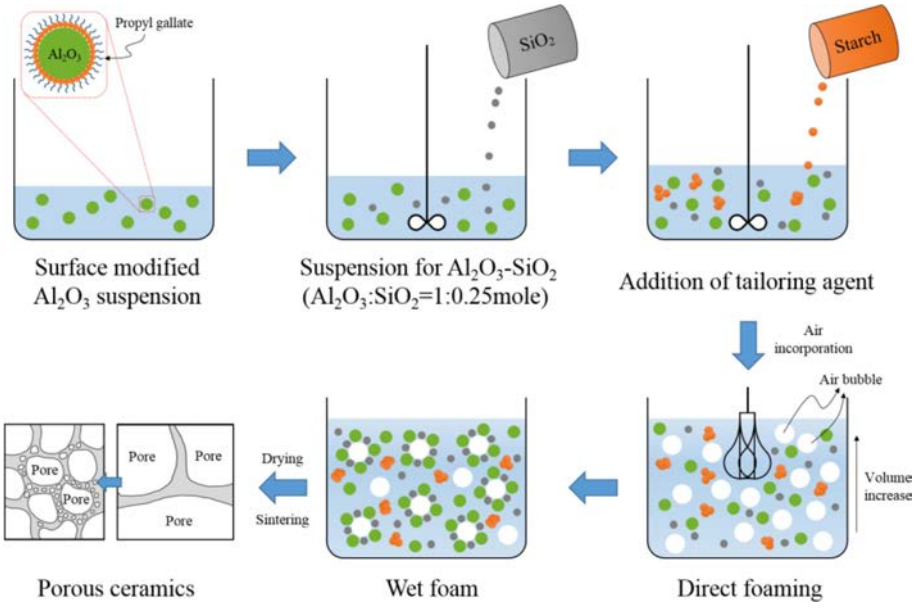

Fig. 1. Schematic diagram of the direct foaming technique to prepare porous Al_2O_3/SiO_2 ceramics.

foaming, and $V_{suspension}$ indicates the volume of suspension before foaming.

The results of the Laplace pressure (ΔP) imply that the difference between the inside and outside pressure of a gas bubble is an important parameter to consider for the stabilization mechanism.

$$\Delta P = \gamma\left(\frac{1}{R_1}+\frac{1}{R_2}\right)=\frac{2\gamma}{R}(Spherical\ bubble) \quad (3)$$

where, γ is the surface tension of the suspension, and R_1 and R_2 are the radii of two interfacing bubbles.

To investigate the wet-foam stability, wet-foam samples were filled into cylindrical molds at a constant volume and were left for 48 hrs. The foam stability was then evaluated by observing the percentage of the volume loss of the foam as follows:

$$Wet\ foam\ stability = \frac{V_{Final}}{V_{Initial}} \times 100 \quad (4)$$

where, V_{Final} indicates the volume of wet foam after 48 hrs, and $V_{Initial}$ indicates the volume of wet foam before 48 hrs.

Average wet bubble size were evaluated by analyzing optical microscope, linear intercept (TU Darmstadt, Germany). The optical microscope (Somtech Vision, South Korea) in transmission mode was connected to a digital camera.

The microstructures of the sintered foams were analyzed by field emission scanning electron microscopy (FESEM) (JEOL, Japan), and characterized the phase composition of the samples by X-ray diffractometry (XRD) (Rigaku D/Max 2500, Japan).

Results and Discussion

Fig. 2 shows the effect of suspension added for the starch on the contact angle and surface tension of the aqueous suspensions. The attachment of particles at gas liquid interfaces occurs when particles are not completely wetted, or in other words, are partially hydrophobic. This enables the production of high volume stable foam, which after drying and sintering, produces porous ceramics. Partially hydrophobic particles remain predominantly in the liquid phase, and exhibit a contact angle $< 90^{o}$. Therefore, measuring the contact angle is an important aspect of the study of foam stability. This graph shows the suspension exhibits contact angles of 66^{o} to 64.5^{o}, which enables good wet foam stability, as this range indicates partial hydrophobization of particles has taken place. It was observed that for all the evaluated samples, upon increasing the 5.0 wt% of suspension added starch, the surface tension of suspensions increases from 30 to 43 mM/m. This can be explained by an increase in surface hydrophobicity of the particles with increasing particle concentration.

Fig. 3 establishes the air contents and average bubble

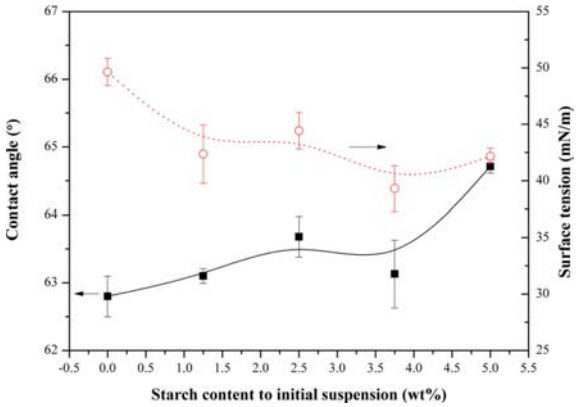

Fig. 2. Contact angle and surface tension of Al_2O_3-SiO_2 suspension with respect to different wt. % of starch content.

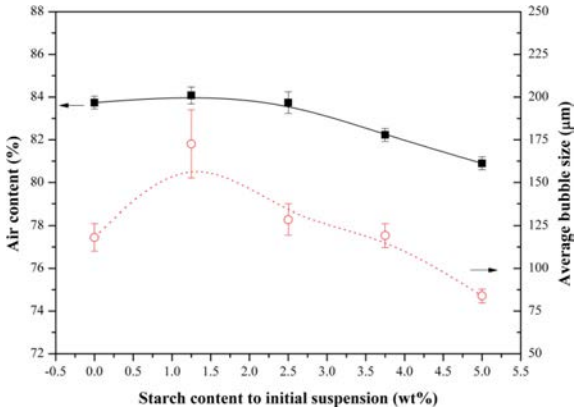

Fig. 3. Air content and average bubble size of Al2O3-SiO2 suspension with respect to different wt. % of the starch content.

size of Al_2O_3-SiO_2 suspension, with respect to different wt. % of starch content added. High volume foams with air content up to 84.2% form upon mechanical frothing, which strongly indicates the stabilization of air bubbles, due to the attachment of particles to the air-water interface. Average bubble size was evaluated, and it was observed that with the addition of 5.0 wt% suspension, the average bubble size suddenly decreased by up to 80 μp. This is probably due to the high viscosity of the suspension, due to higher starch concentration. Whereas, 1.25, 2.5, and 5.0 wt. % of addition enhanced the foam stability, which might be explained by the optimum surface hydrophobicity being achieved, due to the increased starch concentration.

Fig. 4 establishes the relationship between adsorption free energy corresponding to the foam stability, with respect to the different wt.% of suspension added. The adsorption free energy plays an important role in stabilizing foams. By replacing part of the gas-liquid interfacial area, particles that are attached to the gas-liquid interfaces of foams lower the system free energy. The lowest adsorption free energy of 2.45×10^{-12} J resulting from spontaneous bubble growth leads to foam stability of about 75%. The investigated samples exhibit a much higher adsorption free energy of about

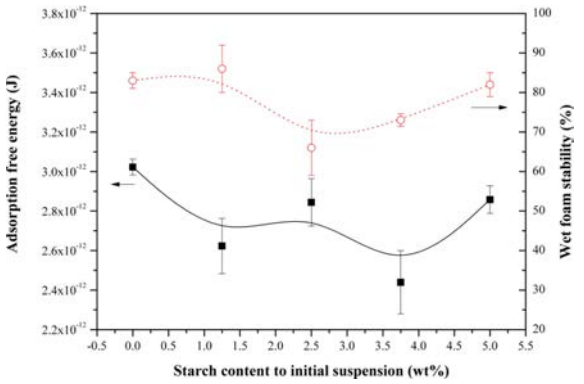

Fig. 4. Adsorption free energy and foam stability of Al_2O_3-SiO_2 suspension with respect to different wt.% of the starch content.

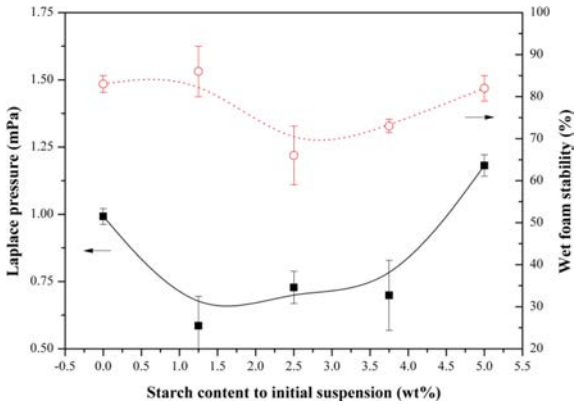

Fig. 5. Laplace pressure and bubble size of Al_2O_3-SiO_2 suspension with respect to different wt.% of the starch content.

2.88×10^{-12} J to 3.4×10^{-12} J at the interface, resulting in irreversible adsorption of particles at the air-water interface, which provides outstanding stability.

Fig. 5 shows the wet foam stability corresponding to the Laplace pressure exerted by the bubbles with respect to the starch content in the colloidal suspension. In this experiment, bubbles were found almost spherical with narrow size distribution. Smaller bubbles are under higher pressure than larger ones, which results in gas diffusion from smaller to larger bubbles, leading to the collapse. As it can be seen, the moderate wet foam stability of 68% was found when the Laplace pressure is 0.73 mPa. The outstanding wet foam stability ranging from 86 to 82% was obtained when the Laplace pressure was about 1.52 and 1.48 mPa respectively. The degree of particle hydrophobization influences the average bubble size of the resultant foams (Fig. 3). This is due to the decrease in surface tension and increases in foam viscosity [14, 16]. This reduces the resistance of air bubbles against rupture and results in the production of foams with average bubble sizes.

Fig. 6 shows the relative increment bubble size with respect to time, where after 1hr, the bubbles tend to collapse due to Ostwald ripening, with a gradual increase in the bubble size. A mixture of Al_2O_3/SiO_2

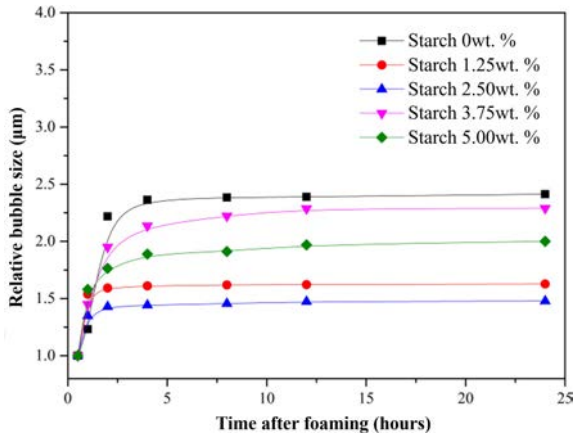

Fig. 6. Relative bubble size of Al_2O_3-SiO_2 suspension with respect to the time after direct foaming.

(1 : 0.25 mole ratio) porous ceramics showed the maximum relative increase in bubble size after 3hr. The initial suspension with the starch consolidation of 1.25 and 2.5 wt. % was found to most stable due to the high wet foam stability (see Fig. 5) as well as the relative bubble size is also relatively stable in all range of time; whereas, it was found the starch contents of 3.75 and 5.0 wt. % to be unstable, with a drastic increase in the bubble size with the increase in time which is the phenomenon occurred by the collapse of smaller bubbles into larger bubbles which is typical destabilization mechanism of Ostwald ripening.

Fig. 7 show a tri-modal hierarchical microstructure of sintered porous ceramics, which were harmonized by moderate-sized pore larger than 300 μm, and small-sized pores in walls of 5 ~ 10 μm. and attribute these to the moderate-sized pores and small-sized voids originating from air bubbles by direct foaming, and the elimination of starch particles during sintering, respectively [17]. When the ceramic-starch foams are heated, the starch granules swell by water absorption, decreasing the available free water. Thus, the ceramic particles, usually of smaller size than the starch granules, locate together in the interstitial space and consolidate into a solid body [18].

Fig. 7 shows the microstructure of the Al_2O_3-SiO_2 based porous ceramics sintered at 1300 °C/for 1 hr. The open/interconnected pores with the pore size of 300 μm in average was found with different wt% of the starch consolidation. On comparing the microstructure image with Fig 3. the narrow bubble size with better wet foam stability (see Fig. 4) was found with the suspension with the 1.25 and 2.5 wt% of the starch consolidation and thus obtained bubble size was about 84 μp but as the heat treatment was done with the dry foams thus produced the bubble were converted to pores with the higher increment which is due to the effect of Ostwald ripening and when the ceramic-starch foams are heated, the starch granules swell by water absorption, decreasing the available free water. Thus, the ceramic

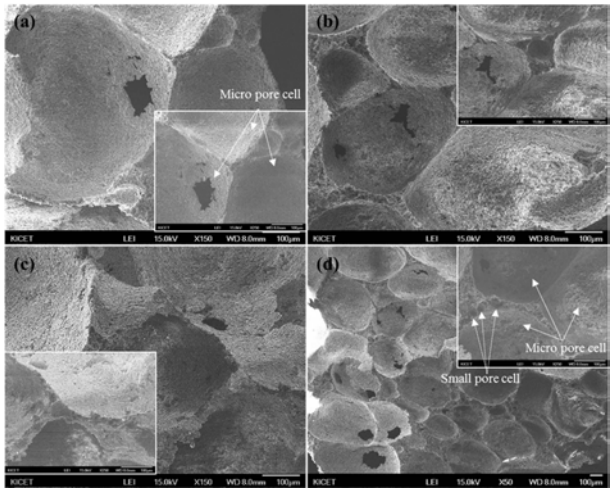

Fig. 7. FESEM image of Al_2O_3-SiO_2 porous ceramics by direct foaming with respect of starch content (a) 0 wt%, (b) 1.25 wt%, (c) 3.75 wt%, and (d) 5 wt% sintered at 1300 ºC.

particles, usually of smaller size than the starch granules, locate together in the interstitial space and consolidate into a solid body [18]. This increases the porosity of the porous ceramics thus produced leading to the varieties of the application field.

The narrow size distribution of macro pores ceramics was controlled by increasing the starch contents and thick struts (films in wet foams), which leads to higher stable wet foams sintered to porous ceramics with a shrinkage of 26-33%. Generally, highly stable wet foam from colloidal suspension leads to a final fine microstructure of porous ceramics containing uniform cell sizes and cell windows. A structure with moderately-sized evenly-interconnected cells is derived as the porosity increases. In this case, the cell morphologies are almost spherical cells, for porosities with increasing starch contents varying from 60 to 35% with a bulk density of 0.95 ~ 1.65 g/cm^3.

Conclusions

With the starch consolidation in a particle-stabilized colloidal suspension through direct foaming, the microstructure of the wet foam is well-tailored to the open/interconnected porous ceramics. The initial colloidal suspension of Al_2O_3-SiO_2 is partially hydrophobized by the propyl gallate (PG), and the suspension was consolidated with starch. The results show a wet-foam stability of more than 80% with a corresponding air content of 70%, Laplace pressure in the range of 0.4 to 0.6 mPa and adsorption free energy of 2.45×10^{-12} J with the consolidation of starch. The uniform distribution of the open/interconnected pores could be controlled with an increment of the starch consolidation, and this leads to the higher stability of the wet foam. The stable wet foam on sintering gave porous ceramics with the pore size up to 300 μm. With porosity up to 60% and the bulk density of 0.95 ~ 1.65 g/cm^3. The pores thus tailored are found to be highly interconnected and open. The Al_2O_3-SiO_2 ceramics thus produced will be applicable as a filter, grinding materials, separation membrane and much more to meet the global trend.

Acknowledgments

This research was financially supported by Hanseo University, Korea.

References

1. M. Scheffler, and P. Colombo, Cellular Ceramics: Structure, Manufacturing, Properties and Applications. P 645. Weinheim, Wiley-VCH, Verlag GmbH & Co. KGaA (2005).
2. N. Sarkar, J.G. Park, S. Mazumder, and I.J. Kim, Ceramics International (2015) 6306-6311.
3. B.P. Binks, Curr. Opin. Colloid Interface Sci. **7** (2002) 21- 41.
4. S. Bhaskar, J.G. Park, S.W. Kim, H.T. Kim, and I.J. Kim, Journal of the Ceramic Society of Japan 123[6] (2015) 1-5.
5. B.S. Murray, Curr. Opin. Colloid Interface Science 12 (2007) 231-241.
6. T.S. Horozov, Curr. Opin. Colloid Interface Science 13 (2008) 134-140.
7. O. Lyckfeldt and J.M. F. Ferreira, J. Eur. Ceram. Soc. 18 (1998) 131-140.
8. T.N. Hunter, R.J. Pugh, G.V. Fanks, G.J. Jameson, Adv. Colloid Interface. Sci. 13[7] (2008) 57-81.
9. P.J. Wilde, Curr. Opin. Colloid Interface. Sci. 5 (2000) 176-181.
10. N. Sarkar, J.G. Park, S. Mazumder, D.N. Seo, and I.J. Kim, Ceramics International 41 (2015) 4021-4027.
11. U.T. Gonzenabach, A.R Studart, E. Tervoort and L.J. Gauckler, Langmuir 10 (2006) 983-988.
12. P. Sepulveda, J.G.P. Binner, J. Eur. Ceram. Soc. 19 (1999) 2059-2066.
13. S. Li, C.A. Wang, and J. Zhou, Ceramics International 39 (2015) 8833-8839.
14. E. Gregorova and W. Pabst, J. Eur. Ceram. Soc. 27 (2007) 669-672.
15. D.M.- Alguacil, E. Tervoort, C. Cattin and L.J. Gauckler, J. Colloid Interface Sci. 353 (2011) 512-18.
16. N. Sarkar, J.G. Park, S. Mazumder, I.S. Han, T.H. Lim and I.J. Kim, Journal of European Ceramic Society 35 (2015) 3969-3976.
17. X. Mao, S. Wang, and S. Shimai, Ceramics International 34 (2008) 107-112.
18. M.H. Talou and M.A. Camerucci, J. Eur. Ceram. Soc. 35 (2015) 1021-1030.